

ORIGINAL ARTICLE

Preservation of groove mark striae formed by armoured mud clasts: The role of armour sediment size and bed yield stress

Carys Lock¹ | Miranda Reid¹ | Jaco H. Baas¹  | Jeff Peakall² 

¹School of Ocean Sciences, Bangor University, Wales, UK

²School of Earth and Environment, University of Leeds, Leeds, UK

Correspondence

Jaco H. Baas, School of Ocean Sciences, Bangor University, Menai Bridge, Wales LL59 5AB, UK.

Email: j.baas@bangor.ac.uk

Funding information

Equinor, Grant/Award Number: 4503099966

Abstract

Striated grooves in tool marks are common at the base of sandstones, especially in deep-marine successions, but their use in physical-process and environmental reconstruction is underdeveloped. To fill this gap in knowledge, striations in the central groove of chevron marks and in chevron-less groove marks were formed in the laboratory by dragging tools armoured with silt, sand or gravel across muddy substrates. These experiments simulated the formation of striated grooves by armoured mud clasts carried at the base of quasi-laminar and fully laminar debris flows, aiming to: (1) delineate the bed shear strengths for the formation of striated grooves at different armour sediment sizes; (2) examine how the preservation potential of striated grooves depends on clay bed rheology and size of armour sediment and (3) discuss how the pre-lithification clay bed consolidation state and size of armour sediment can be reconstructed from striated grooves in the geological record. The experimental results revealed that tools with small-diameter silt and sand armours dragged along soft beds lack striations or, at best, leave poorly defined striations, whereas firm beds and gravel armours exhibit well-defined striations. The spacing of striations formed by gravel clasts corresponds well with the clast diameter, implying that striation spacing is a good proxy for the diameter of armoured gravel under natural conditions. In contrast, the spacing of striae formed by sand armours is greater than the grain diameter, suggesting that the spacing of fine striations can only be used to predict a maximum armour sand size. A comparison of different processes of formation of armoured mud clasts demonstrated that the armouring of mud clasts most probably happens after incorporation of the clasts by erosion into the head of the debris flow and subsequent movement across a loose sandy or gravelly bed surface.

KEYWORDS

armoured mud clast, bed yield stress, striae prominence, striated groove

This is an open access article under the terms of the [Creative Commons Attribution](https://creativecommons.org/licenses/by/4.0/) License, which permits use, distribution and reproduction in any medium, provided the original work is properly cited.

© 2024 The Author(s). *The Depositional Record* published by John Wiley & Sons Ltd on behalf of International Association of Sedimentologists.

1 | INTRODUCTION

Elongate sedimentary structures at the base of sandstone beds have been used routinely for reconstructing palaeocurrent directions since the 19th century (Hall, 1843). Known generically as sole marks (Dżułyński & Sanders, 1962; Peakall et al., 2020, 2024), these structures can be formed by: (a) flow-induced scouring, mostly resulting in flute marks (Crowell, 1955; Allen, 1968, 1984; Dżułyński & Walton, 1965; Enos, 1969; Collinson et al., 2006); (b) flow-induced deformation of a soft substrate, generating, for example, longitudinal ridges and furrows (Craig & Walton, 1962; Dżułyński & Walton, 1965; Anketell et al., 1970) and ‘dinosaur leather’ structures (Chadwick, 1948) and (c) objects in the flow that interact with the substrate, forming continuous tool marks, for example, groove and chevron marks (Shrock, 1948; Kuenen & Sanders, 1956; Dunbar & Rodgers, 1957; Kuenen, 1957; Dżułyński & Ślaczka, 1958; Dżułyński & Walton, 1963; Collinson et al., 2006) and discontinuous tool marks, for example, skip, skim and prod marks (Dżułyński & Ślaczka, 1958; Wood & Smith, 1958; Dżułyński et al., 1959; Allen, 1984). Palaeocurrent direction can be reconstructed from asymmetrically shaped sole marks; these include flutes, ‘scaled’ longitudinal furrows (Craig & Walton, 1962; Dżułyński & Walton, 1965), chevron marks and prod marks. Sole marks that lack asymmetry, such as groove, skip and skim marks, allow quantification of the orientation (i.e. two directions at 180° angles to each other) of the current that formed these structures.

In addition to their widespread use in palaeocurrent analysis, the type and shape of sole marks can also be

linked to the type of flow by which they formed and the rheology of the substrate. With increasing flow cohesion and decreasing flow turbulence, sole marks change from flute marks via discontinuous tool marks (skim to skip to prod mark) to chevron and groove marks, with the continuous tool marks typically generated by quasi-laminar plug flows (sensu Baas et al., 2009) and fully laminar plug flows (sensu Peakall et al., 2020). McGowan et al. (2024) found experimentally that continuous tool marks change with increasing yield stress of a muddy substrate from cut chevron mark (with a narrow, central cut) via interrupted chevron mark (with a wider, central groove and a progressively increasing angle between the chevrons and the central groove) to chevron-less groove marks, thus uncovering a continuum between chevrons and grooves not recognised previously (Figure 1).

Grooves in interrupted chevron marks and in chevron-less groove marks regularly contain striations parallel to the long axis of the groove (Figure 2). These striations can be interpreted to have formed by the asperities of irregularly shaped clasts, and by mud clasts armoured with gravel or sand particles, if the parallel striae are abundant and closely spaced (Peakall et al., 2020; McGowan et al., 2024). The tools are rarely present at the termination of tool marks, but the densely striated grooves provide indirect evidence for the presence of armoured mud clasts in the formative flows as well as the upstream origin of these mud clasts and their armour (McGowan et al., 2024). The particle size of the armour sediment may indicate a local origin of this sediment if the sedimentary succession in which the striated groove occurs contains sediment particles of a similar size. In contrast, if the armour sediment is coarser than the locally deposited

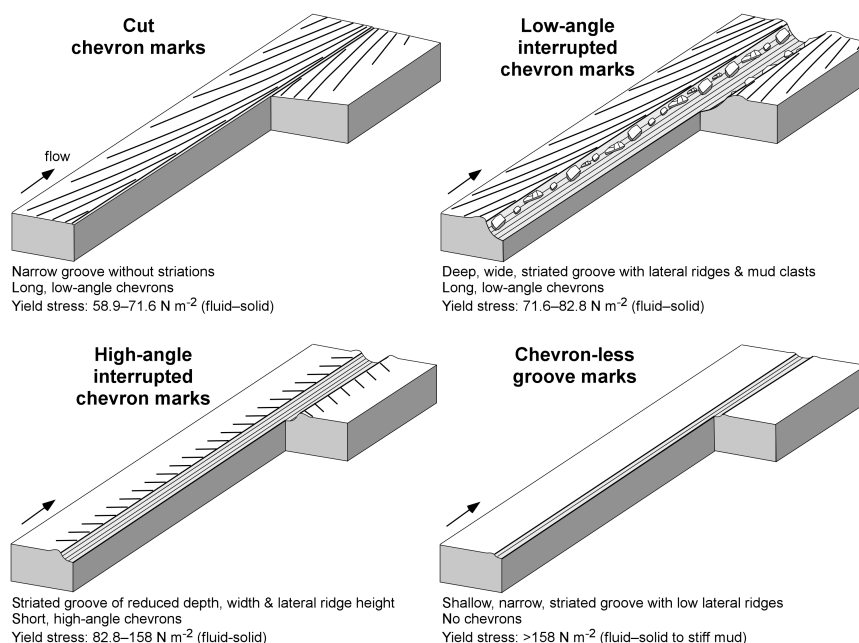


FIGURE 1 Principal types of chevron and groove marks and their relationship with bed rheology. After McGowan et al. (2024).

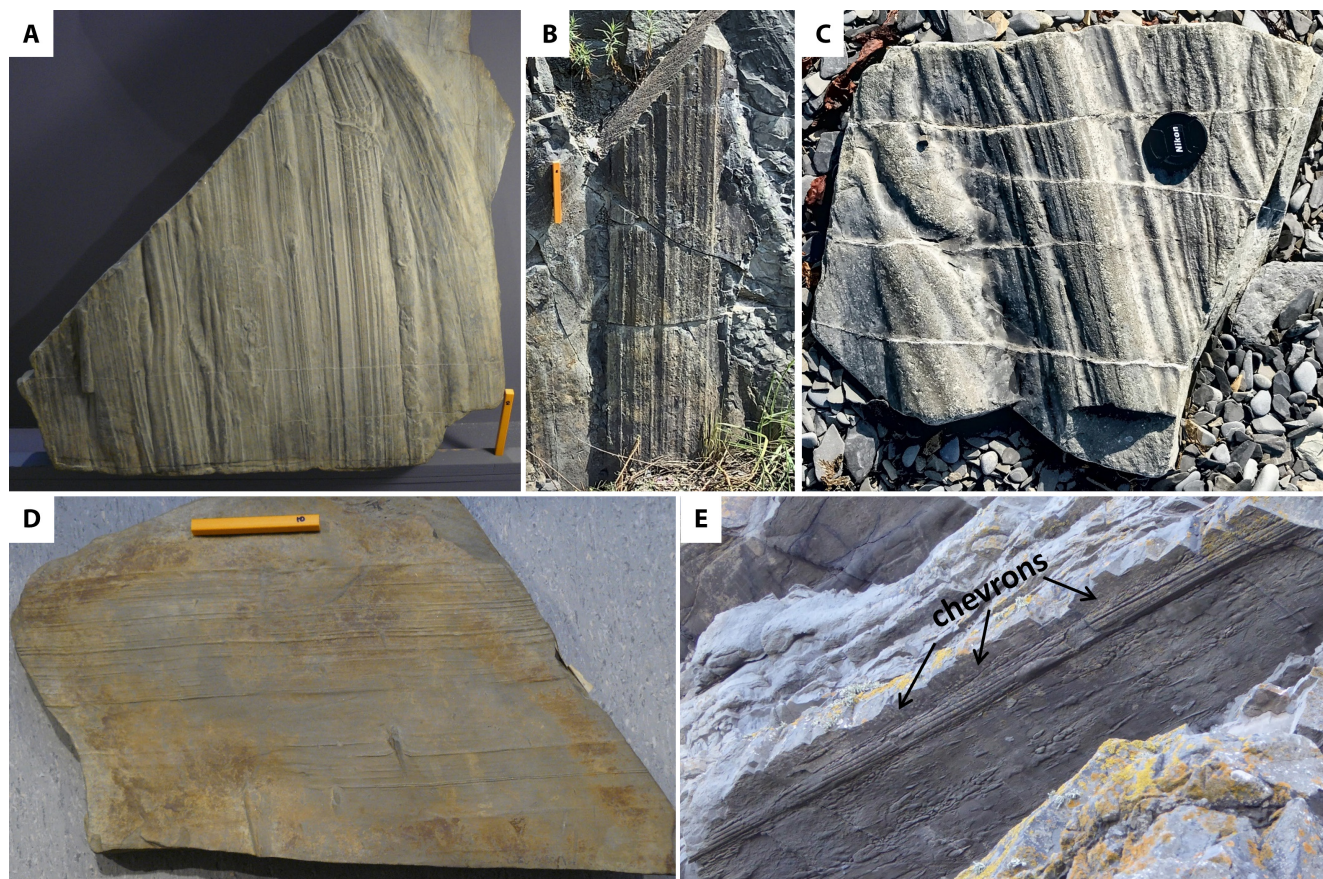


FIGURE 2 Examples of tool marks with striations. (A) Dense group of striated grooves. Oligocene Podhale flysch, Bialy Dunajec, Poland. Sample from the collection of the Natural Sciences Education Centre at the Jagiellonian University, Kraków. Yellow scale bar is 100 mm long. (B) Widely spaced striations in sand-filled groove mark. Lower Carboniferous turbidites, Braciszów quarry, Poland. Yellow scale bar is 100 mm long. (C) Striations in sand-filled groove. Middle Ordovician Cloridorme Formation, Gaspé peninsula, Quebec, Canada. Lens cap for scale, 77 mm in diameter. (D) Narrow striations. Oligocene Cergowa beds, Komancza, Poland. Sample from the collection of the Natural Sciences Education Centre at the Jagiellonian University, Kraków. Yellow scale bar is 100 mm long. (E) 'Rope'-like low-angle interrupted chevron mark with pronounced widely spaced striations. Silurian Aberystwyth Grits Group, west Wales, United Kingdom. Groove mark is *ca* 0.1 m wide.

sediment, the mud clasts are likely to have picked up the armour from upstream locations with coarser sediment. However, this reconstruction of the origin of the sediment armour from striations in interrupted chevron marks and chevron-less groove marks (and possibly also prod and skim marks, which can also be striated; Dżułyński et al., 1959; Allen, 1984; Peakall et al., 2020) is valid only if a predictable relationship exists between the spacing of striae in striated grooves and the size of particles stuck to the mud clasts. Moreover, the degree of preservation of striations in grooves, herein referred to as striation prominence and continuity to define poorly and well-defined striations, as a function of armour sediment size and bed rheology needs to be known. Prominence describes the abundance of striae—where poor abundance includes isolated striae and small groups of striae—and their uniformity in spacing and depth. Continuity is defined as the length of striae relative to the total length of the tool

mark, where low-continuity striae are relatively short or exhibit interruptions along their length, which in turn reduces the prominence. Herein, it is hypothesised that the striation prominence and continuity are higher for firmer substrates and coarser sediment in the mud-clast armour, because the striae on firm beds are less likely to be eroded by subsequent flows and coarser grains produce deeper and more widely spaced striations.

This hypothesis is tested by means of laboratory experiments in which tools armoured with sediment particles of different diameter were dragged across muddy beds with different yield stresses. The main aims of the research were: (1) to delimit the bed rheological properties for the generation of striated groove marks at different armour sediment sizes; (2) to investigate the effect of clay bed rheology and size of armour sediment on the prominence and continuity of striated groove marks and (3) to establish how the experimental data can be used to assess the

pre-lithification clay bed consolidation state (via bed rheology) and size of armour sediment from striated groove marks in the geological record.

Informed by these research aims, six objectives were defined: (a) to conduct tool-drag experiments across water-kaolinite mixtures covering bed yield stresses at which interrupted chevron marks (relatively soft beds) and chevron-less groove marks (relatively hard beds) form (McGowan et al., 2024), as a proxy for the formation of striations by dense, laminar sediment gravity flows; (b) to find the lower yield stress limit for the formation of identifiable striated grooves, assuming that striae do not form in mud that is too water-rich and by sediment armour that is too fine-grained; (c) to compare the prominence and continuity of the striations as a function of clay-bed consolidation state and size of armour sediment; (d) to determine under which conditions the spacing of striations is representative of the size of the armour sediment that produced the striations; (e) to describe how bed consolidation state and size of armour sediment can be reconstructed from striae in natural interrupted chevron marks and chevron-less groove marks and (f) to discuss under which flow conditions armoured mud clasts are formed and how these clasts then generate striated grooves.

2 | METHODOLOGY

The formation of striated chevron and groove marks by armoured mud clasts, as generated by quasi-laminar and fully laminar debris flows under natural conditions (Baas et al., 2009; Peakall et al., 2020), was simulated in the Hydrodynamics Laboratory of the School of Ocean Sciences, Bangor University, by dragging a spherical object covered in sand or gravel across a muddy bed in a rectangular tank. The tank is 0.115 m wide, 0.674 m long and 0.153 m high (Figure 3), and it was filled to approximately one-quarter of its depth (*ca* 0.04 m) with a homogeneous mixture of kaolin clay (Whitchem China Clay Polwhite E Powder; median grain size, $D_{50}=0.009$ mm; density, $\rho_s=2600$ kg m⁻³) and natural seawater (density, $\rho_w=1027$ kg m⁻³), sourced from the Menai Strait next to

the laboratory and filtered before use. Subsequently, the clay surface was flattened with a sharp-edged scraper that covered the width of the tank (without changing the consolidation state of the bed) and, finally, seawater was added to a height of *ca* 0.14 m. Fifteen experiments were conducted using three bed bulk densities: 1413.6, 1439.5 and 1612.2 kg m⁻³ (Table 1), equivalent to water contents of 75.4, 73.8 and 62.8%, and yield stresses, τ_y , of 74.4, 91.3 and 274.7 N m⁻², which characterise low-angle interrupted chevron marks, high-angle interrupted chevron marks and chevron-less groove marks (McGowan et al., 2024), respectively. The yield stresses were calculated from the bed bulk densities using the rheological data of Baker et al. (2017; their table 2). The object used in the experiments was a sphere filled with wet sand and a continuous layer of sand or gravel was glued onto the sphere (Figure 4) to mimic an armoured mud clast. The sphere had a mass of *ca* 0.15 kg and a diameter of 0.05 m. Four sizes of armour sediment were used: well sorted, silt to very fine sand (S-VFS; $D_{50}=0.067$ mm), very well sorted, very fine to fine sand (VFS-FS; $D_{50}=0.123$ mm), very well sorted, coarse sand (CS; $D_{50}=0.552$ mm) and well-sorted gravel ($D_{50}=4.16$ mm). A smooth sphere without armour was used in a control experiment at $\tau_y=91.3$ N m⁻².

In each experiment, the armoured sphere was attached to a fishing reel by a thin wire attached to a threaded bolt (Figure 3) and then placed carefully on the bed, allowing it to penetrate the mud under its own weight. A near-constant dragging velocity across the muddy bed of 74 ± 22 mm s⁻¹ was maintained, so each experiment lasted *ca* 8 s. This velocity guaranteed that the clast stayed in contact with the bed continually. After each experiment, the seawater was siphoned out of the tank at a rate that was sufficiently low to prevent bed disturbance. Thereafter, the tool mark was documented using digital photography and the LiDAR 3D scanning function on an iPhone 13 Pro, and a calliper gauge was used to record a vertical profile of the tool mark perpendicular to the dragging direction at a horizontal and vertical resolution of 5 and 0.5 mm, respectively.

The LiDAR function on an iPhone 13 Pro was used to form digital elevation models (DEMs) of the striated

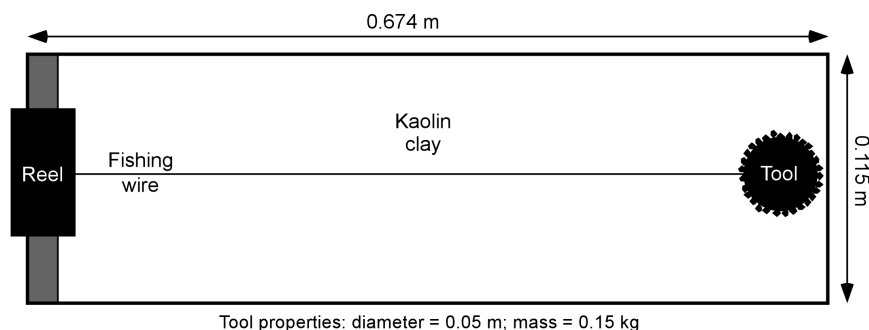


FIGURE 3 Schematic drawing of the experimental setup as seen in planform. The tool was dragged from right to left.

grooves produced by the armoured tools. Subsequently, Agisoft Metashape and Metashape Viewer software, which allow three-dimensional visualisation and dimensional analysis of DEMs, were used to measure the mean spacing of all striations in each groove (Table 1). High-resolution digital photographs of the striations were used to validate the DEM-derived spacing measurements.

The striae prominence was represented quantitatively by standard deviation of the mean of the striation spacing. The striae continuity was subdivided into longitudinal continuity and transverse coverage. The longitudinal continuity was expressed as the mean length, $\overline{C_L}$, of all striations in a groove mark over a groove-parallel distance, d_L , of 0.1 m, converted to percentage of maximum striation length:

$$\overline{C_L} = \frac{1}{n} \sum_{i=1}^{i=n} 100 \frac{C_{L,i}}{d_L} \quad (1)$$

where n is the number of striations and $C_{L,i}$ is the length of striation i (Table 1). Equation (1) shows that grooves with fully continuous striations have a longitudinal continuity of 100%, and the presence of discontinuous striations reduces $\overline{C_L}$ to below 100%. The transverse coverage, C_T , was estimated by determining the percentage of the groove width covered by striations, with 100% denoting a groove fully occupied by striae (Table 1).

3 | RESULTS

3.1 | Visual description of tool marks and striae

The experimental data reveal significant differences in the preservation of striae in the continuous tool marks as a function of armour sediment size and bed yield stress (Figure 5). In the control run, a well-defined groove without striae was produced upon dragging the smooth tool through the bed at $\tau_y = 93.1 \text{ N m}^{-2}$.

3.1.1 | Striated grooves at $\tau_y = 74.4 \text{ N m}^{-2}$

At the lowest bed density, with $\tau_y = 74.4 \text{ N m}^{-2}$, all armoured tools produced low-angle interrupted chevron marks (Figure 1; McGowan et al., 2024) with well-defined, 7–10 mm deep, central grooves. However, except for the experiment with the gravel-armoured tool, the walls of the grooves were more prone to collapse than in the experiments conducted at the same bed density by McGowan et al. (2024), exemplified by the presence of soft mud clasts in the grooves made by the S-VFS and CS-armoured

tools in Figure 5. The S-VFS-armoured tool did not produce any visible striae. In the groove created by the VFS-FS-armoured tool, only some striae were visible. The CS-armoured tool produced more pronounced striae that were more continuous and more often occurred in groups than for the VFS-FS-armoured tool. The groove formed by the gravel-armoured tool contained clear striae that were further apart than those generated by the CS-armoured tool (Figure 5).

3.1.2 | Striated grooves at $\tau_y = 93.1 \text{ N m}^{-2}$

The armoured tools produced high-angle interrupted chevron marks (Figure 1; McGowan et al., 2024) with up to 14 mm deep grooves and well-defined lateral ridges at $\tau_y = 93.1 \text{ N m}^{-2}$, and the striae in the grooves were more prominent than at $\tau_y = 74.4 \text{ N m}^{-2}$. The striae associated with the gravel and CS armours were markedly deep and evenly grouped (Figure 5), compared to the striae at $\tau_y = 74.4 \text{ N m}^{-2}$. The striae created by the VFS-FS-armoured tool were less obvious, that is, discontinuous and covering only part of the width of the groove. The S-VFS-armoured tool produces some striations at this bed yield stress, but these were irregular and poorly developed (Figure 5).

3.1.3 | Striated grooves at $\tau_y = 274.7 \text{ N m}^{-2}$

The bed was firm at $\tau_y = 274.7 \text{ N m}^{-2}$, leading to the formation of shallow (up to 3 mm deep) and narrow chevronless groove marks (Figure 1; McGowan et al., 2024). As at $\tau_y = 93.1 \text{ N m}^{-2}$, the S-VFS-armoured tool created discontinuous, poorly developed striae. The striae formed by the VFS-FS-armoured tool were clearer, but the visually most conspicuous striae were present in the grooves produced by the CS and gravel-armoured tools, albeit slightly less well-developed than at $\tau_y = 93.1 \text{ N m}^{-2}$ for the gravel-armoured tool (Figure 5).

3.2 | Trends in striae preservation

Figure 6 shows degree of striae preservation as a function of median size of armour sediment and bed yield stress, subdivided qualitatively in ‘no striations’, ‘poorly defined striations’, ‘medium-well defined striations’ and ‘well-defined striations’. Grooves with poorly defined striations include all cases where striations are rare, discontinuous and poorly grouped, with a maximum longitudinal continuity, $\overline{C_L}$, and transverse coverage, C_T , of 50% (Table 1). The ‘medium-well defined’ category comprises

TABLE 1 Experimental parameters.

Run	Bed bulk density kaolinite (kg m ⁻³)	Yield stress (N m ⁻²)	Armour grain size (mm)	Tool mark type	Striae prominence	Mean striae width and SD (mm)	Striae longitudinal continuity (%)	Striae transverse coverage (%)
1	1413.6	74.4	4.16	LAICM	Good	3.86 ± 1.64	96	100
2	1413.6	74.4	0.552	LAICM	Medium	0.80 ± 0.16	73	80
3	1413.6	74.4	0.067	LAICM	None	—	0	0
4	1439.5	91.3	4.16	HAICM	Good	3.84 ± 0.97	99	100
5	1439.5	91.3	0.552	HAICM	Good	0.83 ± 0.46	94	100
6	1612.2	274.7	4.16	CLGM	Good	—	—	—
7	1439.5	91.3	0.067	HAICM	Poor	—	<10	<10
8	1612.2	274.7	0.552	CLGM	Good	0.65 ± 0.10	98	100
9	1439.5	91.3	None	HAICM	No striae	No striae	No striae	No striae
10	1612.2	274.7	0.067	CLGM	Poor	—	<10	<10
11	1413.6	74.4	0.067	LAICM	None	—	0	0
12	1413.6	74.4	0.123	LAICM	Poor	—	>10	ca. 50
13	1439.5	91.3	0.123	HAICM	Medium	0.59 ± 0.20	54	50–80
14	1612.2	274.7	4.16	CLGM	Good	4.49 ± 0.57	95	100
15	1612.2	274.7	0.123	CLGM	Medium	0.61 ± 0.11	89	60–90

Abbreviations: CLGM, chevron-less groove mark; LAICM/HAICM, low/high-angle interrupted chevron mark; SD, standard deviation.



FIGURE 4 Examples of spherical tools with sediment armour used in the experiments. The diameter of each sphere is 0.05 m. From left to right: Tool with silt to very fine sand armour, tool with coarse sand armour and tool with gravel (pebble) armour.

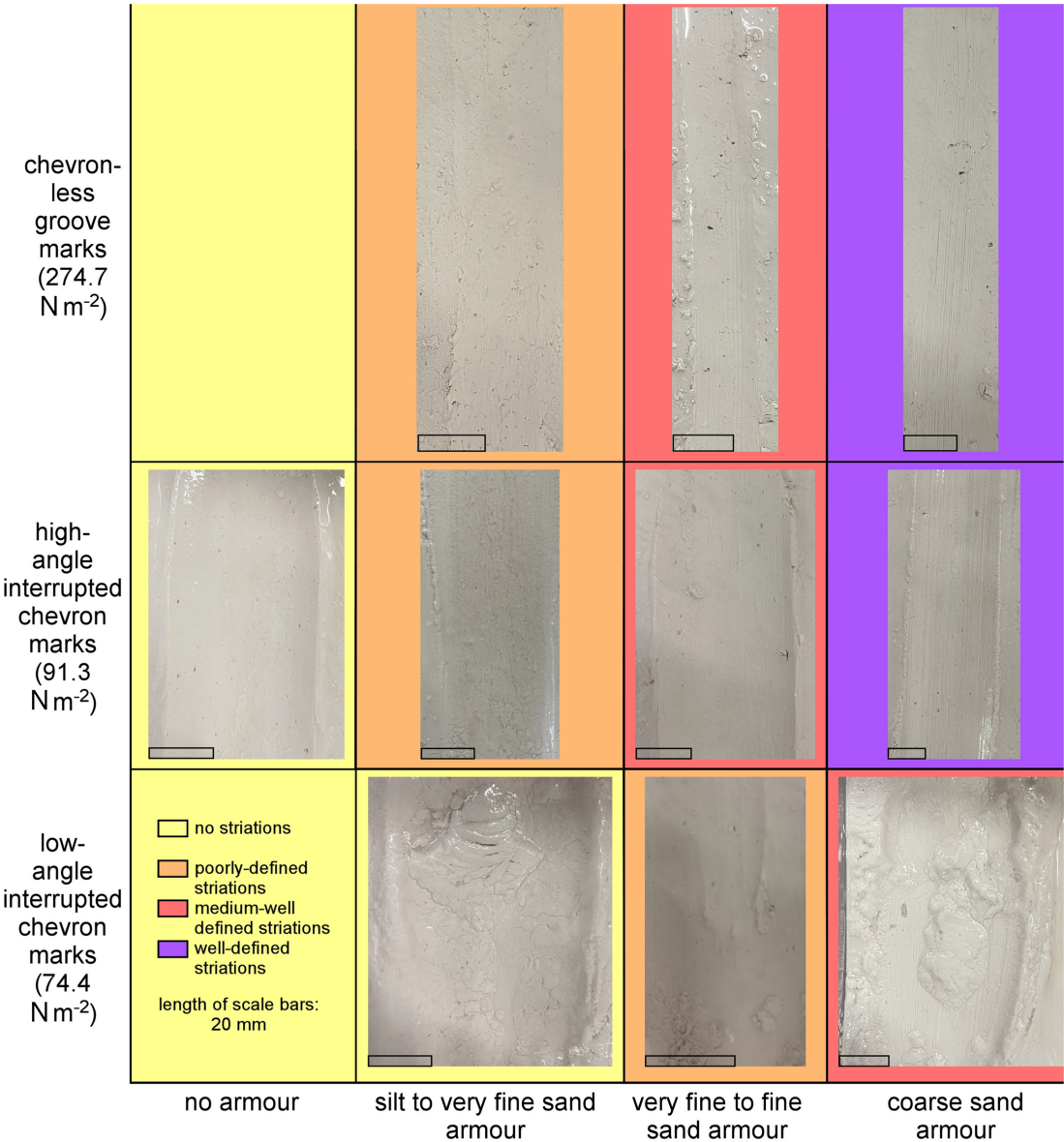


FIGURE 5 Photographic images of continuous tool marks subdivided according to armour sediment size and tool mark type. Note that bed yield stress increased from low-angle interrupted chevron marks to chevron-less groove marks. Colours behind pictures indicate nominal differences in striae prominence, which decreased as armour sediment size and bed yield stress were decreased.

striations that cover most of the width of the grooves, but not all striae can be traced along the full length of the grooves, with $\overline{C_L}$ and C_T ranging from 50 to 90% (Table 1).

Well-defined striations are classified as continuous, and, with few exceptions, they extend across the entire width of the groove, with $\overline{C_L} > 90\%$ and $C_T > 90\%$ (Table 1).

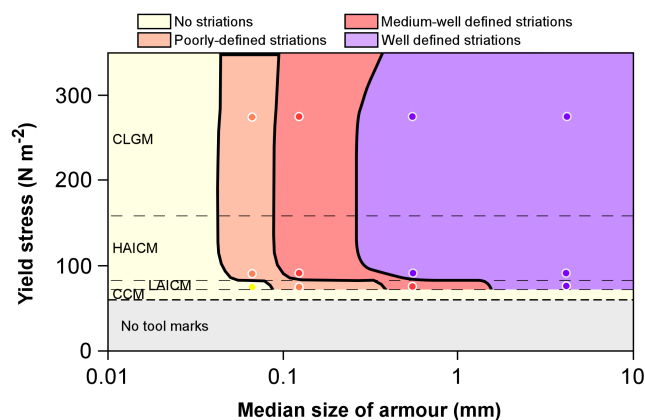


FIGURE 6 Median size of sediment armour against bed yield stress, showing that the most prominent striated grooves form in gravel and coarse sand and for bed yield stresses between *ca* 100 and 300 N m^{-2} . CCM, cut chevron mark; CLGM, chevron-less groove mark; LAICM/HAICM, low/high-angle interrupted chevron mark.

For all bed yield stresses, the striae preservation increased, as the median size of the armour sediment was increased (Figure 6). The gravel and CS armours produced mainly well-defined striations, whereas the VFS-FS and S-VFS armours were dominated by medium-well-defined and poorly defined striations, respectively. This is supported quantitatively by a sharp decrease in the longitudinal continuity (between 95 and 99% to <10%) and transverse coverage (from 100% to <10%) of the striae, as the armour sediment size was decreased (Table 1). The striae formed by the CS and VFS-FS armours became better-defined rapidly from $\tau_y = 74.4 \text{ N m}^{-2}$ (low-angle interrupted chevron marks) to $\tau_y = 274.7 \text{ N m}^{-2}$ (chevron-less groove marks), partly because the grooves were less prone to collapse at 91.3 N m^{-2} and 274.7 N m^{-2} (cf., McGowan et al., 2024). In quantitative terms, the longitudinal continuity and transverse coverage of the striations formed by the CS increased from 73 to 98% and from 80 to 100%, respectively (Table 1). Corresponding increases for the VFS-FS armour were from <10 to 89% and from 50 to 60–90%. All striations formed by the gravel armour were well-defined, with 100% transverse coverage and up to 99% longitudinal continuity (Table 1). However, a small decrease in longitudinal continuity from 99 to 95% was measured between $\tau_y = 91.3 \text{ N m}^{-2}$ and $\tau_y = 274.7 \text{ N m}^{-2}$, after the bed was changed from soft to firm, shown in Figure 6 by a small shift in the striae definition boundaries to coarser armour sediment.

3.3 | Striae spacing

The mean spacing of the well-developed striations produced by the gravel armour was between 3.84 mm and

4.49 mm (Table 1), which is of the same order of magnitude as 4.16 mm, the median diameter of the gravel clasts. Standard deviations of the mean striae spacing for the gravel armour ranged from 0.57 to 1.64 mm (equivalent to 13–42% of the mean). The mean spacing of the striae formed by the CS armour ranged from 0.65 to 0.83 mm, with standard deviations of between 0.10 mm and 0.20 mm (equivalent to 15%–55% of the mean). These spacings are larger than 0.552 mm, the median grain diameter of the CS (Table 1). The VFS-FS armour produced medium-well defined striae with spacings of $0.59 \pm 0.20 \text{ mm}$ for $\tau_y = 91.3 \text{ N m}^{-2}$ and $0.61 \pm 0.11 \text{ mm}$ for $\tau_y = 274.7 \text{ N m}^{-2}$, with these standard deviations equivalent to 34 and 18% of the mean, respectively. As for CS, the mean spacing is larger than 0.123 mm, the median grain diameter of the VFS-FS armour. The spacing of poorly defined striae made by the VFS-FS armour in the softest bed, and the S-VFS armours in all beds could not be measured with sufficient accuracy.

4 | DISCUSSION

4.1 | Process interpretations

The experimental data support McGowan et al. (2024) in that striated grooves are produced by clasts with asperities, but the present study builds upon these findings by revealing novel relationships between the preservation potential and spacing of striations and the rheology of the bed and the size of the sediment particles attached to mud clasts (cf., Peakall et al., 2020). In general, tools with small-diameter silt and sand armours dragged along soft beds lack striations or, at best, leave poorly defined striations, whereas firm beds and gravel armours exhibit well-defined striations (Figure 5). In terms of continuous tool-mark type, it is therefore inferred that low-angle interrupted chevron marks are less likely to exhibit longitudinally continuous striations with full transverse coverage than high-angle interrupted chevron marks and chevron-less groove marks (Figure 6; Table 1). Moreover, the spacing of striations formed by gravel armours corresponds more closely to the diameter of the gravel clasts than those formed by coarse and fine sand armours (Table 1). Soft, water-rich clay beds, here with $\tau_y = 74.4 \text{ N m}^{-2}$, apparently need deep and widely spaced striations formed by tools with coarse sediment armour, here CS to gravel, to prevent the substrate from partially or fully restoring a smooth groove by infilling of the striae behind the moving tool. This process involves shear-induced breaking of the bonds between the kaolinite particles, thus a decrease in the viscosity of the substrate, in turn facilitating flow of the shear-thinning kaolinite–water mixture (cf., Philippe et al., 2011; McGowan et al., 2024). On a larger scale, this

process promotes failure of the wall of the grooves of low-angle interrupted chevron marks, leading to partial coverage of the striations by mud clasts (cf., McGowan et al., 2024). Moreover, the surface of tools covered in silt to fine sand is inferred to be too smooth to fully preserve striations in chevron and groove marks (Figure 5). For tools with coarse sediment armour dragged along firm beds, here with $\tau_y = 274.7 \text{ N m}^{-2}$, the striations in chevron-less groove marks may also not be fully developed (Figure 6). The high yield stress and high viscosity of the bed may prevent the particles from penetrating far enough into the bed to produce well-defined striations. This matches the shallow depth and small width, compared to the tool diameter, of the grooves in these substrates (Figures 5 and 6).

4.2 | Striation preservation and spacing as a proxy for substrate yield stress and armour sediment size

McGowan et al. (2024) showed experimentally that the type of continuous tool mark is a proxy for bed rheology, which the present study expands on by incorporating the preservation potential of striations within grooves. Low-angle interrupted chevron marks, formed at $\tau_y = 71.6\text{--}82.8 \text{ N m}^{-2}$, have long chevrons that are oriented at a sharp angle to the groove (Figure 1), but any striations in the groove are expected to be predominantly longitudinally and transversally discontinuous (Table 1). If present, full preservation of striations in low-angle interrupted chevron marks is most likely indicative of mud clasts armoured with gravel clasts. On the other hand, the presence of longitudinally and transversally discontinuous striations in the grooves of high-angle interrupted chevron marks, exhibiting short chevrons at a wide angle to the groove and formed at $\tau_y = 82.8\text{--}158 \text{ N m}^{-2}$ (Figure 1), and in chevron-less groove marks, formed at $\tau_y > 158 \text{ N m}^{-2}$ (Figure 1), suggests that these striations were formed by mud clasts with a relatively fine-sandy armour (Table 1). Fully preserved striations in these tool mark types are most likely produced by mud clasts with a relatively coarse-sandy or gravelly armour.

McGowan et al. (2024) also found that the width of grooves in interrupted chevron marks and chevron-less groove marks is a poor indicator of the size of the tools that produced the grooves, because the depth of penetration of tools depends on the bed rheology and the submerged mass of the tool. This raises the question if a similar limitation exists for the sediment armour surrounding mud clasts. Intuitively, the depth of penetration of sediment particles in the armour decreases as the firmness of the clay substrate, and thus the time of bed consolidation,

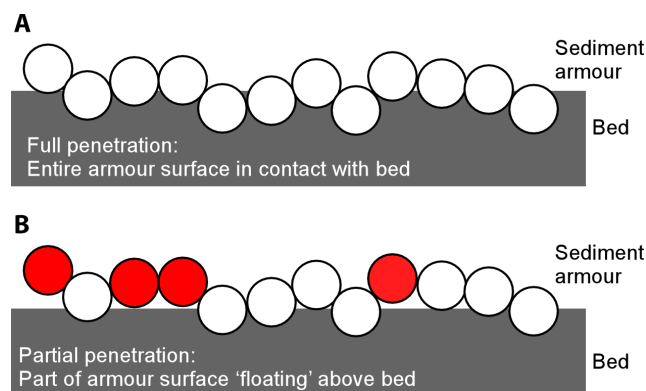


FIGURE 7 Schematic representation of (A) full and (B) particle penetration into the bed of an armoured mud clast. When dragged along the surface (perpendicular to the drawings), the mean striation spacing for full bed penetration is smaller, and closer to the particle size of the sediment armour, than for partial bed penetration, as more particles are in contact with the bed. In (B), the red particles do not form striations.

increases. Moreover, coarse particles should penetrate less far into firm substrates than fine particles. Figure 7 shows conceptually that a shallower depth of penetration causes more widely spaced striations. The influence of substrate firmness on bed penetration explains the small increase in mean striation spacing formed by the gravel armour dragged through the firm substrate, compared to the softer substrates (Run 14 in Table 1) and the lack of such a trend for the sand armours. It is possible that the bed yield stresses used in the experiments were too low to significantly reduce the depth of penetration, but this would have required a hard mud, following the clay-bed type classification scheme of van Rijn (1993), in turn needing an unrealistically long period of continuous bed consolidation under natural conditions of years to centuries (van Rijn, 1993). It is therefore concluded that depth of penetration did not play a major role in controlling striation spacing, and that mostly the entire surface of the sediment armours was in contact with the bed whilst the tools moved through the tank in most experiments.

4.3 | Effect of packing properties of sediment armour particles on striation spacing

The experiments showed that the mean spacing of the striations formed by the gravel armour is similar to the median diameter of the gravel clasts. In contrast, the mean striation spacing of the sand armours is larger than the median diameter of the sand grains, with this difference increasing from CS to VFS-FS (Table 1). As mentioned above, this may be caused by the difference

in preservation potential between striations formed by gravel and sand. Implicit in this interpretation is that there is a perfect match between particle size and striation spacing under full striation preservation. This assumption is not necessarily valid, because this relationship depends on the packing properties of the particles at the edge of the armour. These properties include the packing density and lattice deficiencies that cause certain particles to extend further from the tool than other particles (Figure 7). Random packing densities are more likely than regular, for example, cubic and tetrahedral, packing densities under natural conditions. Further analysis of the effect of packing properties on striation spacing is therefore confined to random packing.

The influence of the packing of sediment armour particles on striation spacing was investigated experimentally by emptying a bag of spheres, each 0.05 m in diameter, in a cylindrical container, 0.3 m in diameter. This resulted in a loose-randomly packed volume of spheres with an irregular upper surface (Figure 8A). In a second experiment, the container was gently shaken afterwards to obtain a denser random packing of spheres. In both experiments, photographs were then taken at 12 different angles in a plane parallel to the upper surface of the sphere-filled container to record 12 curves of maximum sphere extension (black lines in Figure 8B). Subsequently, these curves were used to artificially produce striated grooves by ‘dragging’ the curves towards the photographer (Figure 8C). The next steps involved

measuring the spacing of the striations and calculating the mean spacing for each viewing angle. Finally, the 12 spacings were averaged (and the standard deviation of mean spacing calculated) and then divided by the diameter of the spheres, D_s , to derive a measure for the theoretical striation preservation factor, S_t :

$$S_t = \frac{\bar{W}}{D_s} \quad (2)$$

where \bar{W} is the mean striation spacing for both random-packing experiments (Figure 8). These experiments showed similar values for S_t for the loose and dense-random packing runs, $S_t = 0.89 \pm 0.15$ and $S_t = 0.88 \pm 0.18$, respectively, suggesting that the density of random packing does not have a significant influence on the striation preservation factor.

A mean S_t -value of 0.89 ± 0.16 was used to determine the expected mean striation spacing, \bar{W}_t , in the tool-mark experiments, resulting in $\bar{W}_t = 3.70$ mm for the gravel armour, $\bar{W}_t = 0.491$ mm for the CS armour, $\bar{W}_t = 0.109$ mm for the VFS–FS armour, and $\bar{W}_t = 0.059$ mm for the S–VFS armour. Subsequently, the measured striation preservation factor, S_m , was calculated for each experimental run, using the measured mean spacing of the striations, \bar{W}_m and \bar{W}_t :

$$S_m = \frac{\bar{W}_t}{\bar{W}_m} \quad (3)$$

and plotted as a function of armour sediment size in Figure 9.

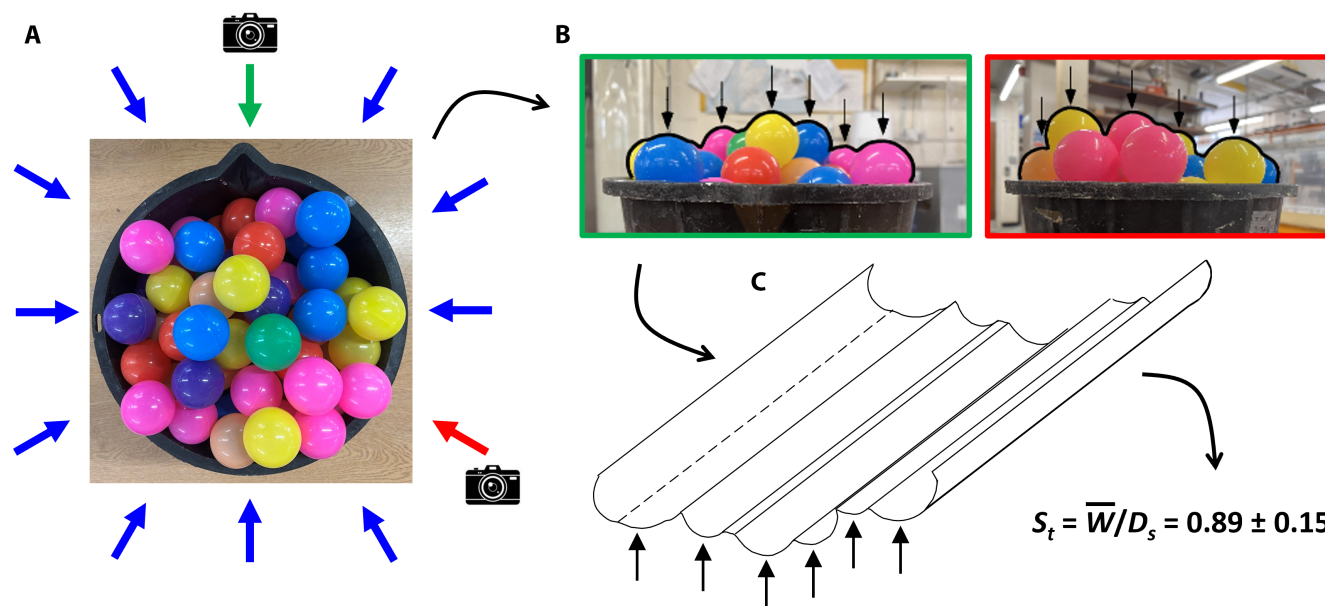


FIGURE 8 Summary of methodology for determining the theoretical relationship between armour sediment size and striation spacing. (A) Loose-randomly packed volume of spheres. Arrows show 12 positions of camera for taking side-view photographs of surface of stack of spheres. Green and red arrows correspond to positions of camera in (B). (B) Shows outline of surface of stacked spheres (black lines) and the positions of maximum extension of spheres (black arrows). (C) Artificial groove for photograph outlined in green in (B), with black arrows showing troughs of striations. S_t = theoretical striation preservation depth; \bar{W} = mean striation spacing; D_s = sphere diameter = 0.05 m.

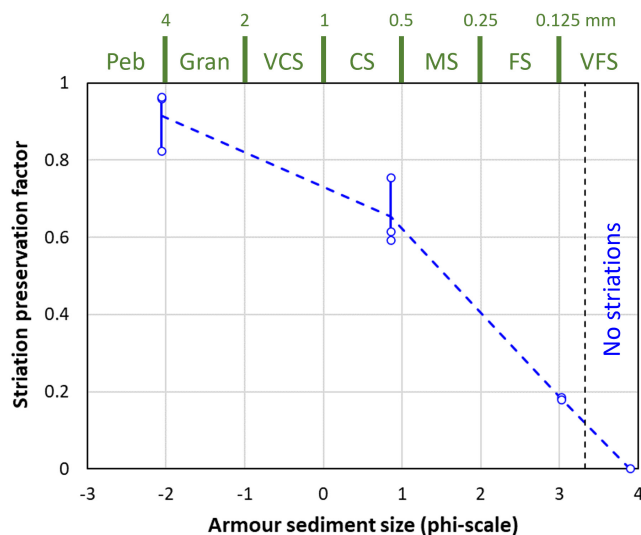


FIGURE 9 Measured striation preservation potential against armour sediment size. CS, coarse sand; FS, fine sand; Gran, granules; MS, medium sand; Peb, pebbles; VCS, very coarse sand; VFS, very fine sand.

Figure 9 shows a rapid decrease in S_m , as the armour sediment size is reduced from gravel to very fine sand, limited by $S_m \approx 0.9$, that is, a good match between armour sediment size and mean striation spacing, for gravel armours and $S_m \approx 0$, that is, no preservation of striations, for very-fine sand armours. This confirms the earlier inference that striation spacing is a good measure for the size of sediment armour only for gravel-sized clasts, and that sandy armours produce striations that are significantly further apart than the size of the sand grains. Because mean striation spacing is unlikely to be smaller than the diameter of the particles in the armour, \overline{W}_m -values smaller than 2 mm, the boundary between sand and gravel, can be used only to determine the maximum size of the sandy armour of mud clasts. This analysis also showed that bed yield stress had no predictable influence on S_m , and therefore on \overline{W}_m (Table 1), for each armour sediment size.

The relative standard deviation of mean striation spacing lies within a similar range for all armours: 13–42% for gravel, 15–55% for CS and 18–34% for VFS–FS. Interestingly, the lower end of these ranges agrees well with the relative standard deviation of \overline{W}_t of 18%. There is a tendency for these low relative standard deviations to occur on firmer beds (Table 1), which confirms that on softer beds most of the variance in the striation spacings is caused by a poorer preservation of individual striae.

4.4 | Interpreting bed rheology and armour size

The results of the present study can be used to aid the interpretation of striated grooves in interrupted chevron

marks and groove marks in terms of bed rheology and armour sediment size. Low-angle interrupted chevron marks with well-developed striae in the central groove are most likely formed by the movement of mud clasts with a gravel armour along a soft substrate, unless the striation spacing is significantly less than 2 mm, but such striations are expected to have smaller longitudinal continuity and transverse coverage. Figure 2E shows an example of a low-angle interrupted chevron mark with a pronounced striated central groove from the Aberarth section of the Silurian deep-marine Aberystwyth Grits Group in west Wales, United Kingdom (Baas et al., 2021). The striations have a spacing of *ca* 0.02 m, thus within the size range of pebbles. The Aberarth section contains a prominent submarine channel fill with various sandy and gravelly facies (Baas et al., 2021; their figure 11B) and abundant mud clasts in hybrid event beds formed in a channel-lobe transition zone (Baas et al., 2021; their figure 10A). The mud clasts armoured with pebbles that formed the striations may therefore have had a local origin. Figure 2E also shows that the striations do not vary considerably in spacing. This suggests that the pebbles were of uniform size and covered the entire surface of the mud clast that was in contact with the low-yield stress substrate.

The spacing of striations in the central groove of high-angle interrupted chevron marks and chevron-less groove marks should be a good indicator of a firm substrate, the presence of gravel in the armour of the mud clast, and the median size of the gravel, if the mean striation spacing is larger than 2 mm. Figure 2B shows an example of a chevron-less groove mark with pronounced striations from Lower Carboniferous turbidites in the Braciszów quarry near the Czech border in southern Poland. These striations are spaced at *ca* 0.01 m on average, suggesting that these were formed by mud clasts with a pebble armour dragged along a firm bed. In contrast to the continuous tool mark in Figure 2E, pebbles are rare in the quarry, indicating that these gravel-armoured mud clasts were derived from an updip location and the debris flows that carried these clasts largely bypassed this depositional site. The striations in the hand specimen shown in Figure 2A, from the Oligocene Podhale flysch, Bialy Dunaj, southern Poland, have a mean spacing of 0.01 m. It is therefore likely that these striations were formed by a mud clast—or several mud clasts, given that the surface is completely covered with striations—with a pebbly armour.

For striations less than 2 mm apart in high-angle interrupted chevron marks and chevron-less groove marks, the sediment armour may have consisted of relatively coarse sand (possibly in the range from fine to very coarse sand), and the mean spacing provides an upper boundary for the median size of this armour. The striations in

Figure 2D from the Oligocene Cergowa beds, Komancza, south-eastern Poland, are mostly less than 1 mm apart (yet, showing a few striations up to 2.5 mm apart). The incomplete transverse coverage of fine striations in this specimen, in addition to the relatively large variation in striation spacing, matches their inferred formation by a relatively fine sandy armour, but it may also point to a softer bed than in the specimen shown in Figure 2A.

4.5 | Prevalence of armoured mud clasts in deep-sea deposits

Although armoured mud clasts have been recognised in both modern (Gutmacher & Normark, 1993; Stevenson et al., 2018) and ancient (Stanley, 1964; Mutti & Normark, 1987; Felix et al., 2009; Dodd et al., 2019; Privat et al., 2021, 2024; Jones et al., 2022; Scarselli, 2024) deep-water sediment, examples are rare compared to striated grooves. This common occurrence of striated grooves in deep-marine deposits has been used to suggest that armoured mud clasts are more prevalent in these settings than previously thought (McGowan et al., 2024). The present work demonstrates that soft substrates and finer-grained armoured clasts leave no trace of striations or, at best, poorly preserved striations. Consequently, this suggests that armoured mud clasts, and particularly those coated in sand, may even be more prevalent than postulated by McGowan et al. (2024).

4.6 | Models for striated groove formation

Striated grooves represent an erosional phase prior to sediment deposition. Furthermore, as argued by Peakall et al. (2020), grooves are formed by clasts being dragged through a substrate whilst held in place by a flow with considerable matrix strength. Thus, grooves represent the product of quasi-laminar plug flow or laminar plug flow (*sensu* Baas et al., 2009; Peakall et al., 2020), equivalent to the intermediate and high-strength debris flows of Talling (2013). The mud clasts in the debris flows must be armoured to produce striated grooves, but how does this process occur? Here, three potential mechanisms are described.

4.6.1 | Long-travelled debris flows

A debris flow might incorporate armoured mud clasts from previous events, as suggested by coatings that

incorporate fossiliferous material from shallow water (Privat et al., 2021), and transport these clasts long distances prior to generating the striated grooves. However, relatively few debris flows traverse entire deep-marine systems, with most transforming to more fluidal flows (Felix & Peakall, 2006; Felix et al., 2009; Spychala et al., 2017), and exotic clasts are unusual coatings of armoured mud clasts in deep-sea sediments.

4.6.2 | Erosion, generation and incorporation of armoured mud clasts into a flow

Mud-clast erosion most likely occurs at the head of a sediment gravity flow, where bed shear stresses are greatest (Necker et al., 2002; Baas et al., 2021). The clasts may then roll across a sand or gravel bed as bedload and become armoured, before being incorporated into a debritic flow component. Physical experiments have shown that the armouring process can be rapid (10 minutes or less: Hizzett et al., 2020) so armouring could happen quickly after the generation of the mud clasts. This armouring process might be close to the location where striated grooves are formed or occur updip where the armour grain size is greater than that in the sediment surrounding the striated grooves, as discussed above. Bedload-transport velocity decreases with increasing clast diameter (Bridge & Dominic, 1984) and is lower than the suspended-load velocity (Baas et al., 2021), suggesting that armoured mud clasts move backwards relative to the flow front. Consequently, in order to act as cutting agents for grooves the armoured clasts would need to be incorporated into the debritic flow component quickly. The paradox here is that there is a need for both an erosive front to generate the clasts and a particulate (sand or gravel) bed for the clasts to roll over. Erosion and associated scouring would need to be initially localised, at or near to the flow front, generating the mud clasts that then become armoured as they travel over uneroded parts of a bed covered in sand or gravel. With increased erosion, the flow front would increase in concentration and cohesion transforming into a debritic head, as argued by Baas et al. (2021), analogous to the high-concentration flow cell observed at the front of the head in modern sediment gravity flows (Azpiroz-Zabala et al., 2017; Pope et al., 2022). This debritic head could then incorporate the armoured mud clasts. This debritic flow component might either rapidly cut the striated grooves or transport the armoured clasts considerable distances prior to striated groove formation.

4.6.3 | Armouring of mud clasts after incorporation of clasts into a debris flow

As described above, the head of a flow may become debritic as a result of rapid erosion and incorporation of both mud clasts and disassociated mud (Baas et al., 2021; Peakall et al., 2024). In many cases, there may be no sand or gravel bed for clasts to roll over, and, as the head becomes more cohesive, clasts may be eroded and incorporated directly into the flow without undergoing bedload transport and thus without undergoing armouring. Mud clasts protrude from the base of the plug in quasi-laminar debris flows downward into a basal laminar fluidal layer, of the order of 10–100 mm thick (Baas et al., 2009; Peakall et al., 2020; McGowan et al., 2024). If the debris flow travels across a sand or gravel bed, these mud clasts may become armoured through incorporation of sediment grains as they are dragged across the substrate. The resulting armoured mud clasts would only have armour on those parts of the clasts that interacted with the substrate, but these are the areas that would act as cutting surfaces if the clasts were subsequently dragged across a mud bed. As the debris flow later traverses cohesive mud beds, the armoured clasts then cut striated grooves. Sediment armouring has been shown to increase the abrasion resistance of mud clasts by up to a factor of four over identical unarmoured clasts (Hizzett et al., 2020). However, given that grain coatings are typically between one and three grain diameters in thickness (Chun et al., 2002), abrasion may partially or completely remove the armour layer, leaving either sparsely armoured clasts or unarmoured clasts prior to the clasts being uplifted into the flow as is known to occur in subaerial debris flows (Johnson et al., 2012; Peakall et al., 2020). The dominant record of these armoured clasts may thus be the striated grooves, without the presence of the clasts themselves.

4.6.4 | Summary: Formative mechanisms

All three mechanisms probably form striated grooves. However, long-travelled debris flows with exotic coated mud clasts are rare in deep-marine systems, and thus are unlikely to be a key mechanism for forming striated grooves. Similarly, direct incorporation of armoured mud clasts into a debritic flow component may be relatively infrequent, given the requirements for erosion of mud clasts, bedload transport across a sand or gravel bed, and rapid incorporation of the clasts into the head of the debris flow. Consequently, armouring of mud clasts that are already in a debritic flow front may be the most frequent mechanism.

4.7 | Opportunities for future research

The present experimental study was conducted with well-sorted and very well-sorted sediment armours that covered the entire surface of a spherical tool. Whilst providing novel information on the use of sole marks in the reconstruction of sedimentary process and bed rheology, this experimental design can be regarded as a simplification of the conditions responsible for forming striated grooves in nature. There are therefore opportunities for future research into, for example, the influence on striation properties of: (i) the degree of sorting of sediment that armours mud clasts; (ii) incomplete armours around mud clasts and (iii) the shape and angularity of mud clasts. Poorly sorted sediment armours would increase the variance of striation spacing, and thus complicate the reconstruction of armour sediment size from striation spacing. However, it is hypothesised that the effect of sediment sorting is relatively small in deep-marine environments, where well-sorted and well-graded turbidites often dominate. Poorly sorted sediment armours would therefore require special conditions, for example, pick up of sediment by soft mud clasts from the top of poorly sorted debris flow deposits or adhesion of sand and gravel to mud clasts within poorly sorted debris flows. Incomplete surficial armours would also complicate the reconstruction of armour sediment size from striation spacing, but this would increase the exposure of mud clasts to more rapid disintegration (Kuenen, 1957; Smith, 1972; Hizzett et al., 2020), thus potentially confining incompletely armoured mud clasts to a local origin. Armoured mud clasts need to be soft and cohesive to facilitate the development of a surficial armour. Such clasts are hypothesised to be more prone to abrasion, and thus have a smoother, more rounded, surface, than firmer, less cohesive mud clasts. The formation of striations by sediment armour and asperities on the same mud clast is therefore less likely than the formation by either process acting alone.

5 | CONCLUSIONS

The present laboratory study reveals novel relationships between the preservation potential and spacing of striations and the rheology of the bed and the size of the sediment particles attached to mud clasts. For all bed yield stresses, the striae preservation increases with increasing median size of the armour sediment. Gravel and coarse-sand armours produce mainly well-defined striations, whereas very-fine sand to fine-sand and silt-to-very-fine sand armours are dominated by medium-well defined and poorly defined striations, respectively. Striations are also better defined on firm beds than soft beds (*sensu van Rijn, 1993*). Low-angle interrupted chevron marks are therefore less likely to

exhibit longitudinally continuous striations with full transverse coverage than high-angle interrupted chevron marks and chevron-less groove marks. Accounting for the grain packing density, the mean spacing of the striations formed by gravel armours is similar to the median diameter of the gravel clasts, but the mean striation spacing of sand armours is larger than the median grain size, with this difference increasing with decreasing grain diameter. Striations more than 2 mm apart are therefore better suited for determining the origin—local or more proximal—of the gravel clasts that form these striations than narrower striations formed by sand armours. Finally, the armouring of mud clasts most likely takes place after bed erosion and entrainment of the clasts into the head of the debris flow, followed by flow across a loose sandy or gravelly bed surface.

ACKNOWLEDGEMENTS

The experimental data presented in this paper were collected by Carys Lock and Miranda Reid as part of the Undergraduate Internship Scheme of Bangor University, Wales/Cymru. The laboratory setup and consumables were funded by a research grant from Equinor, Norway, and the setup was kindly built by Rob Evans. We thank reviewer Carlos Zavala, an anonymous reviewer, and journal editor Peter Swart for their perceptive comments that helped improve this manuscript.

CONFLICT OF INTEREST STATEMENT

The authors have no conflict of interest to declare.

DATA AVAILABILITY STATEMENT

The data that support the findings of this study are available from the corresponding author upon reasonable request.

ORCID

Jaco H. Baas  <https://orcid.org/0000-0003-1737-5688>

Jeff Peakall  <https://orcid.org/0000-0003-3382-4578>

REFERENCES

- Allen, J.R.L. (1968) Flute marks and flow separation. *Nature*, 219, 602–604.
- Allen, J.R.L. (1984) *Sedimentary structures: their character and physical basis*. Amsterdam: Elsevier, p. 1256.
- Anketell, J.M., Cegla, J. & Dżułyński, S. (1970) On the deformational structures in systems with reversed density gradients. *Annales de la Société Géologique de Pologne*, 40, 3–30.
- Azpiroz-Zabala, M., Cartigny, M.J.B., Talling, P.J., Parsons, D.R., Sumner, E.J., Clare, M.A., Simmons, S.M., Cooper, C. & Pope, E.L. (2017) Newly recognized turbidity current structure can explain prolonged flushing of submarine canyons. *Science Advances*, 3, e1700200.
- Baas, J.H., Best, J.L., Peakall, J. & Wang, M. (2009) A phase diagram for turbulent, transitional, and laminar clay suspension flows. *Journal of Sedimentary Research*, 79, 162–183.
- Baas, J.H., Tracey, N.D. & Peakall, J. (2021) Sole marks reveal deep-marine depositional process and environment: implications for flow transformation and hybrid-event-bed models. *Journal of Sedimentary Research*, 91, 986–1009.
- Baker, M.L., Baas, J.H., Malarkey, J., Silva Jacinto, R., Craig, M.J., Kane, I.A. & Barker, S. (2017) The effect of clay type on the properties of cohesive sediment gravity flows and their deposits. *Journal of Sedimentary Research*, 87, 1176–1195.
- Bridge, J.S. & Dominic, D.F. (1984) Bed load grain velocities and sediment transport rates. *Water Resources Research*, 20, 476–490.
- Chadwick, G.H. (1948) Ordovician “dinosaur-leather” markings (Abstract). *Geological Society of America Bulletin*, 59, 1315.
- Chun, S.S., Choe, M.Y. & Chough, S.K. (2002) Armored mudstone boulders in submarine debris-flow deposits, the Hunghae Formation, Pohang Basin: an evidence for the large-scale slumping of adjacent area of a submarine channel or scar wall. *Geosciences Journal*, 6, 215–225.
- Collinson, J., Mountney, N. & Thompson, D. (2006) *Sedimentary Structures*, 3rd edition. Harpenden: Terra Publishing, p. 292.
- Craig, G.Y. & Walton, E.K. (1962) Sedimentary structures and palaeocurrent directions from the Silurian rocks of Kirkcudbrightshire. *Transactions. Edinburgh Geological Society*, 19, 100–119.
- Crowell, J.C. (1955) Directional-current structures from the Prealpine Flysch, Switzerland. *Geological Society of America Bulletin*, 66, 1351–1384.
- Dodd, T.J.H., McCarthy, D.J. & Richards, P.C. (2019) A depositional model for deep-lacustrine, partially confined, turbidite fans: early Cretaceous, North Falkland Basin. *Sedimentology*, 66, 53–80.
- Dunbar, C.O. & Rodgers, J. (1957) *Principles of stratigraphy*. New York: Wiley, p. 356.
- Dżułyński, S. & Sanders, J.E. (1962) Current marks on firm mud bottoms. *Transactions. Connecticut Academy of Arts and Sciences*, 42, 57–96.
- Dżułyński, S. & Ślaczka, A. (1958) Directional structures and sedimentation in the Krosno Beds (Carpathian flysch). *Annales Societatis Geologorum Poloniae*, 28, 205–259.
- Dżułyński, S. & Walton, E.K. (1963) Experimental production of sole markings. *Transactions. Edinburgh Geological Society*, 19, 279–305.
- Dżułyński, S. & Walton, E.K. (1965) *Sedimentary features of Flysch and Greywackes*. Developments in Sedimentology 7. Amsterdam: Elsevier, p. 274.
- Dżułyński, S., Książkiewicz, M. & Kuenen, P.H. (1959) Turbidites in flysch of the Polish Carpathian Mountains. *Geological Society of America Bulletin*, 70, 1089–1118.
- Enos, P. (1969) Anatomy of a flysch. *Journal of Sedimentary Petrology*, 39, 680–723.
- Felix, M. & Peakall, J. (2006) Transformation of debris flows into turbidity currents: mechanisms inferred from laboratory experiments. *Sedimentology*, 53, 107–123.
- Felix, M., Leszczynski, S., Slaczka, A., Uchman, A., Amy, L. & Peakall, J. (2009) Field expressions of the transformation of debris flows into turbidity currents, with examples from the Polish Carpathians and the French Maritime Alps. *Marine and Petroleum Geology*, 26, 2011–2020.
- Gutmacher, C.E. & Normark, W.R. (1993) Sur submarine landslide, a deep-water sediment slope failure. In: Schwab, W.C., Lee, H.J. & Twichell, D.C. (Eds.) *Submarine landslides: selected studies in*

- the U.S. exclusive economic zone. Denver, CO: U.S. Geological Survey, pp. 158–166.
- Hall, J. (1843) *Geology of New York, Part 4, comprising the survey of the Fourth Geological District*. Albany: Charles Van Benthuyson and Sons, p. 683.
- Hizzett, J.L., Sumner, E.J., Cartigny, M.J.B. & Clare, M.A. (2020) Mud-clast armoring and its implications for turbidite systems. *Journal of Sedimentary Research*, 90, 687–700.
- Johnson, C.G., Kokelaar, B.P., Iverson, R.M., Logan, M., LaHusen, R.G. & Gray, J.M.N.T. (2012) Grain-size segregation and levee formation in geophysical mass flows. *Journal of Geophysical Research, Earth Surface*, 117, F01032.
- Jones, G.E.D., Welbon, A.I.F., Mohammadlou, H., Sakharov, A., Ford, J., Needham, T. & Ottesen, C. (2022) Complex stratigraphic fill of a small, confined syn-rift basin: an Upper Jurassic example from offshore mid-Norway. In: Chiarella, D., Archer, S.G., Howell, J.A., Jackson, C.A.-L., Kombrink, H. & Patruno, S. (Eds.) *Cross-border themes in petroleum geology II: Atlantic margin and Barents Sea*, Vol. 495. London: Geological Society, Special Publication, pp. 139–177.
- Kuenen, P.H. (1957) Sole markings of graded greywacke beds. *The Journal of Geology*, 65, 231–258.
- Kuenen, P.H. & Sanders, J.E. (1956) Sedimentation phenomena in Kulm and Flozleeres graywackes, Saverland and Oberharz, Germany. *American Journal of Science*, 254, 649–671.
- McGowan, D., Salian, A., Baas, J.H., Peakall, J. & Best, J. (2024) On the origin of chevron marks and striated grooves, and their use in predicting mud bed density and yield stress. *Sedimentology*, 71, 687–708.
- Mutti, E. & Normark, W.R. (1987) Comparing examples of modern and ancient turbidite systems: Problems and concepts. In: Legget, J.K. & Zuffa, G.G. (Eds.) *Marine clastic sedimentology: concepts and case studies*. London: Graham & Trotman, pp. 1–38.
- Necker, F., Härtel, C., Kleiser, L. & Meiburg, E. (2002) High-resolution simulations of particle-driven gravity currents. *International Journal of Multiphase Flow*, 28, 279–300.
- Peakall, J., Best, J.L., Baas, J.H., Hodgson, D.M., Clare, M.A., Talling, P.J., Dorrell, R.M. & Lee, D.R. (2020) An integrated process-based model of flutes and tool marks in deep-water environments: implications for palaeohydraulics, the Bouma sequence, and hybrid event beds. *Sedimentology*, 67, 1601–1666.
- Peakall, J., Best, J., Baas, J.H., Wignall, P.B., Hodgson, D.M. & Łapcik, P. (2024) Flow-induced Interfacial Deformation Structures (FIDS): implications for the interpretation of palaeocurrents, flow dynamics and substrate rheology. *Sedimentology*. <https://doi.org/10.1111/sed.13219>
- Philippe, A.M., Baravian, C., Imperor-Clerc, M., De Silva, J., Paineau, E., Bihannic, I., Davidson, P., Meneau, F., Levitz, P. & Michot, L.J. (2011) Rheo-SAXS investigation of shear-thinning behaviour of very anisometric repulsive disc-like clay suspensions. *Journal of Physics: Condensed Matter*, 23, 194112.
- Pope, E.L., Cartigny, M.J.B., Clare, M.A., Talling, P.J., Lintern, D.G., Vellinga, A., Hage, S., Açıkalın, S., Bailey, L., Chapplow, N., Chen, Y., Eggenhuisen, J.T., Hendry, A., Heerema, C.J., Heijnen, M.S., Hubbard, S.M., Hunt, J.E., McGhee, C., Parsons, D.R., Simmons, S.M., Stacey, C.D. & Vendettuoli, D. (2022) First source-to-sink monitoring shows dense head controls sediment flux and runout in turbidity currents. *Science Advances*, 8, eabj3220.
- Privat, A.M.-L., Hodgson, D.M., Jackson, C.A.-L., Schwarz, E. & Peakall, J. (2021) Evolution from syn-rift carbonates to early post-rift deep-marine intraslope lobes: the role of rift basin physiography on sedimentation patterns. *Sedimentology*, 68, 2563–2605.
- Privat, A.M.-L.J., Peakall, J., Hodgson, D.M., Schwarz, E., Jackson, C.A.-L. & Arnol, J.A. (2024) Evolving fill-and-spill patterns across linked early post-rift depocentres control lobe characteristics: Los Molles Formation, Argentina. *Sedimentology*, 71, 1639–1685. <https://doi.org/10.1111/sed.13190>
- Scarselli, N. (2024) Exploring the predictive power of seismic geomorphology to assess sedimentary characteristics of gravity-flow deposits: examples from offshore East and West Africa reservoirs. In: Newton, A.M.W., Andresen, K.J., Blacker, K.J., Harding, R. & Lebas, E. (Eds.) *Seismic geomorphology: sub-surface analyses, data integration and palaeoenvironment reconstructions*, Vol. 525. London: Geological Society, Special Publications, pp. 163–168.
- Shrock, R.R. (1948) *Sequence in layered rocks: a study of features and structures useful for determining top and bottom or order of succession in bedded and tabular rock bodies*. New York: McGraw-Hill, p. 507.
- Smith, N.D. (1972) Flume experiments on the durability of mud clasts. *Journal of Sedimentary Petrology*, 42, 378–383.
- Spychala, Y.T., Hodgson, D.M., Prêlat, A., Kane, I.A., Flint, S.S. & Mountney, N.P. (2017) Frontal and lateral submarine lobe fringes: comparing sedimentary facies, architecture and flow processes. *Journal of Sedimentary Research*, 87, 75–96.
- Stanley, D.J. (1964) Large mudstone-nucleus sandstone spheroids in submarine channel deposits. *Journal of Sedimentary Petrology*, 34, 672–676.
- Stevenson, C.J., Feldens, P., Georgiopoulou, A., Schönke, M., Krastel, S., Piper, D.J.W., Lindhorst, K. & Mosher, D. (2018) Reconstructing the sediment concentration of a giant submarine gravity flow. *Nature Communications*, 9, 2616.
- Talling, P.J. (2013) Hybrid submarine flows comprising turbidity current and cohesive debris flow: deposits, theoretical and experimental analyses, and generalized models. *Geosphere*, 9, 460–488.
- van Rijn, L.C. (1993) *Principles of sediment transport in rivers, estuaries and coastal seas*. Amsterdam: Aqua Publications, p. 700.
- Wood, A. & Smith, A.J. (1958) The sedimentation and sedimentary history of the Aberystwyth Grits (Upper Llandoveryan). *Quarterly Journal of the Geological Society*, 114, 163–195.

How to cite this article: Lock, C., Reid, M., Baas, J.H. & Peakall, J. (2024) Preservation of groove mark striae formed by armoured mud clasts: The role of armour sediment size and bed yield stress. *The Depositional Record*, 10, 426–440. Available from: <https://doi.org/10.1002/dep2.309>